Weierstraß-Institut
für Angewandte Analysis und Stochastik
Leibniz-Institut im Forschungsverbund Berlin e. V.

Surfing the edge: Finding nonlinear solutions
using feedback control

Ashley P. Willis[1], Yohann Duguet[2], Oleh E. Omel'chenko[3], Matthias Wolfrum[3]

submitted: April 19, 2017

[1] School of Mathematics and Statistics
University of Sheffield
Hicks Building
Sheffield 7RH
United Kingdom
E-Mail: a.p.willis@sheffield.ac.uk

[2] LIMSI-CNRS
UPR 3251
Université Paris-Saclay
F-91403 Orsay
France
E-Mail: duguet@limsi.fr

[3] Weierstrass Institute
Mohrenstr. 39
10117 Berlin
Germany
E-Mail: oleh.omelchenko@wias-berlin.de
matthias.wolfrum@wias-berlin.de

Surfing the edge: Finding nonlinear solutions using feedback control

Ashley P. Willis, Yohann Duguet, Oleh E. Omel'chenko, Matthias Wolfrum

Abstract

Many transitional wall-bounded shear flows are characterised by the coexistence in state-space of laminar and turbulent regimes. Probing the edge boundary between the two attractors has led in the last decade to the numerical discovery of new (unstable) solutions to the incompressible Navier–Stokes equations. However, the iterative bisection method used to achieve this can become prohibitively costly for large systems. Here we suggest a simple feedback control strategy to stabilise edge states, hence accelerating their numerical identification by several orders of magnitude. The method is illustrated for several configurations of cylindrical pipe flow. Travelling waves solutions are identified as edge states, and can be isolated rapidly in only one short numerical run. A new branch of solutions is also identified. When the edge state is a periodic orbit or chaotic state, the feedback control does not converge precisely to solutions of the uncontrolled system, but nevertheless brings the dynamics very close to the original edge manifold in a single run. We discuss the opportunities offered by the speed and simplicity of this new method to probe the structure of both state space and parameter space.

1 Introduction

In the recent years, there has been increasing evidence for the dynamical importance of exact unstable solutions, such as travelling waves or periodic orbits, for weakly turbulent flows [12, 3, 5, 33]. This is best understood so far for the case of subcritical wall-bounded shear flows, where the base flow is linearly stable at flow rates where turbulence is also sustained. These unstable solutions are the only non-trivial solutions, and are all disconnected from the trivial laminar solution [8].

Most solutions discovered so far appear in saddle-node bifurcations and hence arise in pairs. The solution on the lower energy branch often belongs to the laminar-turbulent separatrix, "the edge", which separates initial conditions that lead to relaminarisation from those that experience transition to turbulence [11, 27]. The attractor within the edge separatrix is labelled the "edge state". When a solution located on the edge has only one real unstable eigenvalue, it acts as an attractor within the edge. It is possible that there may be more than one edge state for a given system. Upper branch solutions are thought to be either embedded in the turbulent attractor, or, together with the lower branch solution, bracket the turbulent dynamics [10].

Knowledge of an invariant solution within the edge has become the first step of a common strategy to unfold the whole bifurcation diagram of the system [18, 2, 23], but identification of exact coherent states remains a demanding task. In the absence of a well-understood sequence of bifurcations from the base flow, i.e. when all classical continuation methods fail [29], several strategies have been employed to find such solutions. The size of the systems under study, usually between 10^4 to 10^9 dimensions, requires specialised iterative strategies, which in particular avoid any operation involving the storage of full matrices. A perhaps more challenging issue is that a good initial guess for the identification is

usually unavailable. During the 1990s and early 2000s, the main strategy used to bypass this issue was homotopy (see e.g. [13]). This relies on an efficient root finder, typically a Newton–Raphson solver coupled to an arc-length continuation algorithm. This method may track the solutions in parameter space around the fold, but does not easily help to identify distinct branches. To apply this method, a companion problem featuring a linear instability of the base flow must first be identified. Once a bifurcated solution is identified, it is continued nonlinearly to a solution of the original problem. Success requires very good intuition for suitable homotopies that might work, plus involves the complexity of solving for the multiple systems. It is also unclear how continued solutions participate in the dynamics.

Later, bisection methods, which make use of timesteppers, began to gain popularity: the amplitude of an arbitrary perturbation to the base flow is rescaled repeatedly, until a trajectory is found which for a sufficiently long time stays away from both the laminar and the turbulent state [11, 27, 24]. Such a trajectory is usually chaotic, but with some luck, if there exists a regular solution with only one unstable eigendirection, there is hope that the bisection algorithm will converge to it [25]. Imposing discrete symmetries to the dynamics often reduces the number of unstable eigendirections of the ECS contained in the associated subspace [7]. As a result the likelihood of identifying symmetry-invariant solutions is increased, but their relevance to the non-symmetric dynamics is uncertain. In the more general case where the edge trajectory is chaotic, recurrence analysis can sometimes identify an approach to a simple state, which can be converged using a good Newton solver, possibly enhanced by some globalisation method [30, 6]. The main drawbacks of bisection methods are the hazardous chances of success, the difficulty to converge interesting recurrent parts of the dynamics using Newton methods, and more importantly their cost. Indeed one bisection requires 2^n individual runs until machine precision ε_M is reached at n^{th} iteration, i.e. $n \sim -log(\varepsilon_M)/log2$, at which point the process needs to be restarted M times as long as no simple edge state has been reached. The total cost is hence of $Mn \geq 100$ runs at least, with the runs getting longer as the accuracy improves. For instance, in [16], each bisection required a total of $Mn \approx 400$ runs, which corresponds to $O(10^6 - 10^7)$ CPU hours. This high cost makes parametric studies infeasible in practice. Other numerical methods have been suggested as alternatives to the bisection-rootfinder combination, e.g. iterative adjoint optimisation methods [9, 19] though they involve significant mathematical and computational complexity. In summary, it is always desirable to find simpler and less expensive alternative methods.

In the present paper we demonstrate how unstable edge states can be found numerically, by introducing into the original system a "control" term that counteracts the edge instability and is able to stabilise unstable states without altering them significantly. This enables the system to dynamically approach the edge state in a single simulation of the controlled system. A key property of a control for this purpose is that it should influence only the stability, not the structure of the *a priori* unknown target, i.e. the control should act as non-invasively as possible. At the same time, it should efficiently force a large set of initial conditions towards the states of interest. Using control as a tool to numerically find and analyse unknown unstable objects in a complex dynamical system has already been successfully applied to a variety of problems. A classical example is the time-delayed feedback control [22] able to stabilise certain periodic orbits provided their period is known. Another example is Selective Frequency Damping, which, by filtering all non-zero temporal frequencies, may stabilise steady state solutions [1]. In the latter case, however, the steady solutions must not possess unstable non-oscillatory eigenvalues [31], which is frequently the case for edge solutions in subcritical shear flows. All these methods are not designed to target the edge manifold.

In this article we propose a remarkably simple linear feedback control, which is able to constrain the dynamics to the edge manifold, and to stabilise invariant solutions that are stable within it. This scheme was recently used in high-dimensional systems of non-locally coupled oscillators to stabilise unstable branches of "chimera" states [26, 34]. In an interesting analogy to shear flows, the chimeras

are metastable chaotic states coexisting with a fully synchronized ("laminar") state [20]. They belong to a folded branch such that the unstable lower branch acts as a separatrix between the synchronous state and the chimera states. The control scheme makes a system parameter μ state-dependent by imposing a linear relation

$$\mu(t) = \mu_0 + \kappa(A_0 - A(t)) \tag{1}$$

between the parameter and an observable $A(t)$. (In the following we will identify μ with Re and A with a component of the perturbation energy.) Stabilisation of a folded branch can be explained using the simplest possible example, a folded branch of equilibria given by the normal form of a saddle-node bifurcation at $\mu = 0$:

$$\dot{x}(t) = \mu - x^2(t). \tag{2}$$

By choosing $A \equiv x$ and applying the constraint (1), the dynamics is restricted to the slanted straight line in a (μ, x) representation, whose slope is given by the control gain κ, see figure 1(right). Intersections of the line (2) with the original branches $x = \pm\sqrt{\mu}$ correspond to equilibria common to both the controlled and the uncontrolled system. A straightforward calculation shows that for suitably chosen control parameters, equilibria on the unstable lower branch can be stabilised. In particular, by varying dynamically the control gain κ, the controlled equilibrium can sweep along the (unstable) lower branch. The constants μ_0 and x_0 determine a pivot point around which the constraint line is rotated. This control is non-invasive provided that A is constant along the controlled orbit, which is the case for e.g. the unstable equilibrium of (2). Controlled trajectories with periodic or chaotic fluctuations in $A(t)$ may still show good quantitative and qualitative agreement with an uncontrolled trajectory for a parameter value near to the time-average $\langle\mu\rangle_t$. The control may be described as non-invasive on average [26]. In this way, it is possible to obtain periodic orbits to be used as initial states for a corresponding Newton solver. Sweeping the control gain may yield an overview of qualitatively different dynamical regimes along the 'global' lower branch, i.e. the edge.
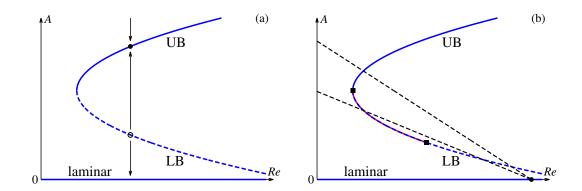

Figure 1: Sketch in an (A, Re) representation of the stability of the uncontrolled (left) and controlled system using the feedback control method (right) based on the constraint (1). The labels 'UB' and 'LB' refer to the upper and lower branch in the uncontrolled system, respectively.

In the present paper we introduce the feedback control method in order to stabilise edge states in the case of cylindrical pipe flow governed by the incompressible Navier–Stokes equations. The plan of the paper is as follows. In Section 2 we present the numerical set-up. In section 3 we apply the control scheme to several different pipe flow cases, first in a restricted domain and then in an extended domain allowing for axial localisation. Finally possible applications for the methods are discussed in the concluding Section 4.

2 Numerical methodology

2.1 Direct numerical simulation of pipe flow

We consider here the case of cylindrical pipe flow with a fixed mass flux. The control parameter μ in Eq. (1) is here the Reynolds number $Re = UD/\nu$, where U is the constant bulk velocity, D the pipe diameter and ν the kinematic viscosity of the fluid. Using U and D as the scales, the non-dimensional laminar state is characterised by an axial velocity profile $\boldsymbol{u}_{\mathrm{lam}}(r) = 2(1 - (2r)^2)\boldsymbol{e}_z$ for $0 \leq r \leq \frac{1}{2}$, driven by a homogeneous pressure gradient $(\partial_z p_{lam})\boldsymbol{e}_z$. The full velocity field $\boldsymbol{u} = (u, v, w)$, which contains the radial, azimuthal and axial components of the velocity, satisfies together with the pressure p the incompressible Navier–Stokes equations at all times :

$$\boldsymbol{\nabla} \cdot \boldsymbol{u} = 0, \tag{3}$$

$$\frac{\partial \boldsymbol{u}}{\partial t} + (\boldsymbol{u} \cdot \boldsymbol{\nabla})\,\boldsymbol{u} = -\boldsymbol{\nabla}p + \frac{1}{Re}\boldsymbol{\nabla}^2\boldsymbol{u}. \tag{4}$$

The flow satisfies the no-slip velocity conditions at the wall. The code ensures that this condition is satisfied to machine precision via the influence matrix method [17]. We advance (4) in time using the hybrid spectral finite-difference code *openpipeflow.org* [32]. The code employs Fourier expansions $\mathrm{e}^{\mathrm{i}(2\alpha kz + mm_0\theta)}$, where k and m are respectively the axial and the azimuthal wavenumbers. This imposes streamwise periodicity with a wavelength $L = \pi/\alpha$ in units D. The integer m_0 indicates the degree of rotational symmetry of the flow field in the azimuthal direction, $m_0 = 2$ refers to a two-fold symmetry while $m_0 = 1$ corresponds to the absence of any discrete rotational symmetry. In some cases we also impose mirror symmetry about the plane $\theta = 0$, $Z\boldsymbol{u} = \boldsymbol{u}$, where

$$Z : (u, v, w, p)(r, \theta, z) \to (u, -v, w, p)(r, -\theta, z), \tag{5}$$

and the shift-and-reflect symmetry $S\boldsymbol{u} = \boldsymbol{u}$, where

$$S : (u, v, w, p)(r, \theta, z) \to (u, -v, w, p)(r, -\theta, z + L/2). \tag{6}$$

In Sections 3.1 and 3.2 we consider simulations with $m_0 = 2$ in domains with respectively $\alpha = 1.25$ and 0.12566. With dealiasing, variables are evaluated on grids in $r \times \theta \times z$ of respectively $64 \times 48 \times 72$ and $64 \times 48 \times 576$ points. In Section 3.3, for $m_0 = 1$ and $\alpha = 1.25$, the resolution is $64 \times 96 \times 72$.

2.2 Implementation of the feedback control

After some experimentation, the following scalar observable was selected for the constraint (1):

$$A(t) = \int_{r=0.35}^{0.5} |\boldsymbol{u}(t) - \boldsymbol{u}_{\mathrm{lam}}|^2 \, r \, \mathrm{d}r \, \mathrm{d}\theta \, \mathrm{d}z \tag{7}$$

where $r = 0.5$ corresponds to the wall. This observable was chosen as a robust precursor to large energy drops or relaminarisation events (many other observables are also possible). Identifying μ with Re, the constraint (1) therefore reduces $Re(t)$ in response to an increase in the amplitude $A(t)$, and increases $Re(t)$ in response to a decrease in $A(t)$.

The factor $1/Re$ appears as the coefficient of the viscous term, which is treated implicitly in the timestepping, and is used in the evaluation of time stepping matrices. Rather than recalculating these matrices every time step, a close reference value Re_r is used for the implicitly treated term. The value

of Re_r is kept with 1% of the actual Re, and the small correction term with coefficient $(1/Re - 1/Re_r)$ is treated explicitly.

Finally, the pivot point is chosen as $(Re_0, A_0) = (10^4, 0)$. Using a large value of Re_0 at first sight suggests that spatial resolution issues may arise for large $Re(t)$. Fortunately, large $Re(t)$ occurs for small energies $A(t)$, for which spectral drop-off is more rapid. Further, the aim is specifically to constrain the dynamics to a particular range of lower energies for a given κ. It has been verified that the drop-off in energy spectra is sufficient that all stabilised states considered in this paper are well resolved.

A relatively slow time-dependence of the control parameter is also introduced in the form

$$\kappa(t) = \kappa_0 \, \mathrm{e}^{t/T} \tag{8}$$

where T is a chosen time-scale constant. From the point of view of convergence to invariant solutions, T should be longer than the decay period of the least-damped mode of a stabilised solution of the controlled system. Since this is unknown, it is simply chosen long relative to the time scale of the intrinsic variability.

3 Results

3.1 Short periodic pipe with m_0=2

We present first the results with the feedback control for a short pipe of length $L = 2\pi/\alpha$ with $\alpha = 1.25$, $m_0 = 2$ and no additional symmetry. This system was considered in [14], and was shown to possess a lower-branch travelling wave (TW) with only one unstable real eigenvalue. It was later verified in [7] that bisection in this system could identify a travelling wave as edge state, but further, that bisection could converge to two travelling waves from different families, depending on the initial condition. We describe now how the feedback controller described in the previous section successfully identified and stabilised another travelling wave solution on the edge.

We start from a turbulent snapshot at $Re = 2000$, then vary $\kappa(t)$ according to (8) with $T = 250$ and $\kappa_0 = 4 \times 10^5$. As shown in figures 2a–b, the time series of $A(t)$ initially displays erratic fluctuations until $t \approx 300 \, D/U$, where the dynamics appears to be smoother and fluctuations are damped. From $(A, Re) \approx (5 \times 10^{-3}, 1800)$ onwards, the backwards fold in figure 2a indicates that the dynamics stays away from the laminar state ($A = 0$) while a lower branch is being captured. At $t = 375 \, D/U$, $\dot{\kappa}$ is set to zero, i.e. $\kappa = \kappa_1 = 4 \times 10^5 \times \mathrm{e}^{1.5}$ (green line in figure 2b). The new trajectory converges towards a fixed point, i.e. a travelling wave solution, with constant A. The associated velocity field in a cross-section is displayed in figure 3(a). While the symmetry was not imposed, the time integration with the control converged to a solution invariant under S, being an S2 state of [14, 21]. It was verified using a Newton-solver that the corresponding solution is also solution to the original uncontrolled Navier–Stokes equations. The linear stability of the states are compared in their eigenspectrum $\{\sigma\}$, calculated using an Arnoldi algorithm, with and without the control ($\kappa = \kappa_1$ and $\kappa = 0$, respectively), figure 3(b), where $Re(\sigma) > 0$ indicates instability. Whereas the TW is unstable in the uncontrolled system, it is stabilised by the feedback control. Applying the control with $\dot{\kappa} < 0$ the simulation also remains on the stabilised lower branch, as demonstrated by the green line in figure 2(left). Sweeps along the lower branch in either direction is therefore a very efficient alternative to numerical continuation with a Newton scheme for rapid numerical continuation of the TW solution in this region.
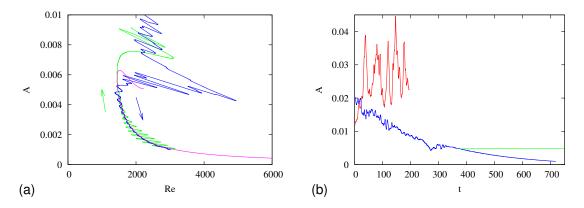
Figure 2: Application of the feedback control with $\alpha = 1.25$ and $m_0 = 2$. (a): (Re, A) representation, control with $\dot{\kappa} > 0$ (blue) and $\dot{\kappa} < 0$ (green), arc-length continuation of the TW (pink). (b): $A(t)$ uncontrolled (red), controlled with unsteady $\kappa(t)$, constant κ for the stabilisation of the TW.

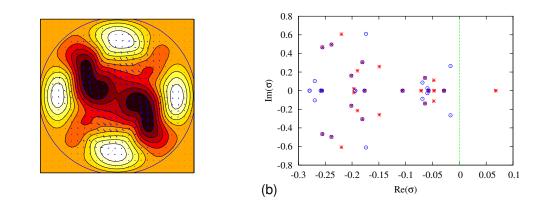Figure 3: (a): Cross section of the stabilised TW solution with $\alpha = 1.25$ and $m_0 = 2$. Streamwise velocity perturbation in colour (from dark to white) and cross-stream components (vectors). (b): Eigenvalue spectrum with (blue circles) and without control (red crosses).

3.2 Long periodic pipe with m_0=2

We consider next the case $L = 25D$ with $m_0 = 2$ and mirror symmetry Z. This system, considered by [2] and later by [4], is known to possess a relative periodic orbit as an edge state, in the form of a weakly modulated travelling wave whose velocity field is axially localised. As in Section 3.1, a simulation starting from a turbulent state at $Re = 1900$ is first used with time-varying $\kappa(t)$ following (8) with $\kappa_0 = 1.62 \times 10^5$ and $T = 400$. Figure 4a shows the dynamics in an (Re, A) representation, where for $A \leq 0.03$ a lower branch has been captured by the scheme. At time $t = 300 \, D/U$ the $\dot{\kappa}$ held fixed with $\kappa_1 = 1.62 \times 10^5 \times e^{0.75}$. Close-ups on the time series of $A(t)$ and $Re(t)$ show weak periodic modulations around steady values, indicating convergence towards a relative periodic orbit (RPO) (figure 4b). The converged RPO has a time-averaged Reynolds number $\langle Re \rangle_t \approx 1450$. A point on this orbit was passed to the Newton solver for the uncontrolled system at $Re = 1450$, and converged in one Newton step. The controlled and uncontrolled RPOs do not exactly coincide, but are close. Figure 4c show a projection in (E_{3d}, β) (observe the scale and distance from the origin), where $E_{3d} = \int |\boldsymbol{u} - \langle \boldsymbol{u} \rangle_{\theta,z}|^2 \, r \, dr \, d\theta \, dz$ and $1 + \beta = \langle \partial_z p \rangle / \partial_z p_{\mathrm{lam}}$. Their periods are respectively 10.67 and 10.61 units D/U. Stabilisation is substantiated in the altered Floquet exponents, displayed in figure 4(d). Unlike for the previous short pipe, where the edge state was a travelling wave solution, the controller has achieved convergence to an RPO, which is not precisely a solution to the uncon-

trolled equations. The control stays approximately non-invasive on average, however, and the isolated solution is close (only a single Newton step was required to go from one solution to the other with a relative error of less than 10^{-6}). It manages this approach in only one short computation for the large system.
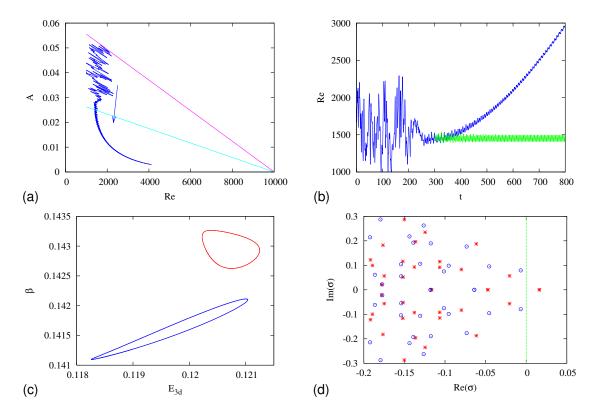

Figure 4: Application of the feedback control with $L = 25D$, $m_0 = 2$ and mirror-symmetry imposed. (a): (Re, A) representation. (b): time series of $Re(t)$ with unsteady (blue) and steady (green) $\kappa(t)$ for the stabilisation of the RPO. (c): Converged RPO converged using the feedback control (red) versus original unstable RPO (blue) at $Re = 1450$ in a (E_{3d}, β) representation. (d): Spectrum of Floquet exponents for the TW solution with (blue circles) and without control (red crosses).

3.3   Short periodic pipe with m_0=1

Bisections in periodic pipes without any rotational symmetry imposed have been performed [24, 7] but to date no edge state with a simple dynamics was reported for $m_0 = 1$. Here we apply mirror symmetry to an $m_0 = 1$ computation in a short pipe with $\alpha = 1.25$. The control by itself did not stabilise any TW solution in this case. A narrow window, however, of unsteady yet quiescent dynamics of the controlled system was identified in figure 5a near the intersection with the indicated straight line. Taking the state at this point as an initial guess in a Newton search converged to a new TW solution at $Re = 2680$, whose cross-section and eigenvalue spectrum are displayed in figures 5b-c, respectively. Note that this new TW does not satisfy the shift-and-reflect symmetry. It is characterised by one real unstable eigenvalue and one pair of complex unstable eigenvalues. Using the control the real eigenvalue is stabilised, and the resulting solution becomes only weakly unstable. Also shown is a cross-section of the solution after numerical continuation to $Re = 1428$ at this $\alpha = 1.25$.
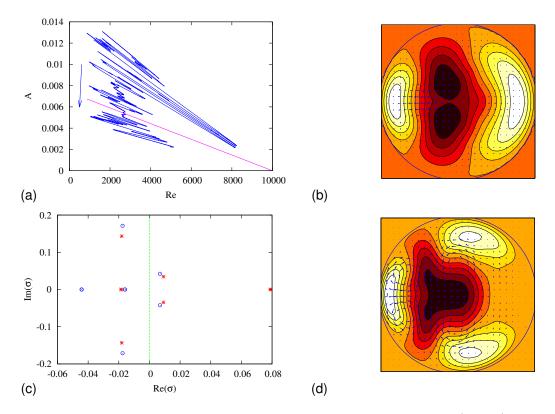
Figure 5: Application of the feedback control with $\alpha = 1.25$, $m_0 = 1$. (a): (Re, A) representation. (b): Cross section of the stabilised TW solution (same colour coding as in figure 3), $Re = 2680$. (c): Eigenvalue spectrum for the TW solution with (blue circles) and without control (red crosses). (d): Cross section after continuation to $Re = 1428$, $\alpha = 1.25$.

4   Conclusions

We have demonstrated that the present feedback control method is able to stabilise invariant solutions that are edge states of the uncontrolled pipe flow system. Stabilised travelling waves correspond to solutions of the uncontrolled Navier-Stokes equations. The control strategy is thus non-invasive only in the case where the edge state of the original system is a travelling wave [26]. Relative periodic orbits or chaotic regimes stabilised using the method, however, are not precisely invariant solutions of the uncontrolled Navier–Stokes equations, but are expected to be sufficiently close for rapid continuation to the original system. In both cases, the feedback control method proves very efficient at bringing the system close to the original edge state in only one short computation, whereas the same task using the bisection method would require $O(100)$ times as many simulations. Coupled with a Newton–Krylov solver, this new method, thanks to its low cost, can be used to probe the bifurcation diagram of the original system and explore the edge manifold without prior bisection. Adapting this method to other parallel shear flows, or to any other spatiotemporal system with hysteresis, is straightforward. A similar feedback control has recently been considered for turbulence in stratified plane Couette flow [28] to attain a target energy. Whilst the target energy might not be commensurate with invariant solutions, not known a priori, and were not isolated for the case of a very large domain, the approach also enables states of much lower target energy to be sustained. Since one run is sufficient to uncover the whole lower branch parametrised by Re (or potentially another parameter such as e.g. α or an additional force), it can either be used to perform wider parametric studies, or to identify the interesting regimes within the edge when multiple bifurcations occur [15]. We therefore recommend implementation of the present control scheme as a simple precursor to the more expensive bisection and complex Newton–

Krylov implementation.

References

[1] ÅKERVIK, ESPEN, BRANDT, LUCA, HENNINGSON, DAN S, HŒPFFNER, JÉRÔME, MARXEN, OLAF & SCHLATTER, PHILIPP Steady solutions of the Navier-Stokes equations by selective frequency damping. *Physics of Fluids* **18** (6), 068102 (2006).

[2] AVILA, MARC, MELLIBOVSKY, FERNANDO, ROLAND, NICOLAS & HOF, BJOERN Streamwise-localized solutions at the onset of turbulence in pipe flow. *Physical Review Letters* **110** (22), 224502 (2013).

[3] CHANDLER, GARY J & KERSWELL, RICH R Invariant recurrent solutions embedded in a turbulent two-dimensional Kolmogorov flow. *Journal of Fluid Mechanics* **722**, 554–595 (2013).

[4] CHANTRY, MATTHEW, WILLIS, ASHLEY P & KERSWELL, RICH R Genesis of streamwise-localized solutions from globally periodic traveling waves in pipe flow. *Physical Review Letters* **112** (16), 164501 (2014).

[5] CVITANOVIĆ, PREDRAG Recurrent flows: the clockwork behind turbulence. *Journal of Fluid Mechanics* **726**, 1–4 (2013).

[6] DUGUET, YOHANN, PRINGLE, CHRIS CT & KERSWELL, RICH R Relative periodic orbits in transitional pipe flow. *Physics of Fluids* **20** (11), 114102 (2008).

[7] DUGUET, Y., WILLIS, A. P. & KERSWELL, R. R. Transition in pipe flow: the saddle structure on the boundary of turbulence. *J. Fluid Mech.* **613**, 255–274 (2008).

[8] ECKHARDT, BRUNO, SCHNEIDER, TOBIAS M, HOF, BJORN & WESTERWEEL, JERRY Turbulence transition in pipe flow. *Annu. Rev. Fluid Mech.* **39**, 447–468 (2007).

[9] FARAZMAND, MOHAMMAD An adjoint-based approach for finding invariant solutions of Navier–Stokes equations. *Journal of Fluid Mechanics* **795**, 278–312 (2016).

[10] GIBSON, JOHN F, HALCROW, JONATHAN & CVITANOVIĆ, PREDRAG Visualizing the geometry of state space in plane couette flow. *Journal of Fluid Mechanics* **611**, 107–130 (2008).

[11] ITANO, T. & TOH, S. The dynamics of bursting process in wall turbulence. *J. Phys. Soc. Jpn.* **70**, 703–716 (2001).

[12] KAWAHARA, GENTA, UHLMANN, MARKUS & VAN VEEN, LENNAERT The significance of simple invariant solutions in turbulent flows. *Annual Review of Fluid Mechanics* **44**, 203–225 (2012).

[13] KERSWELL, RR Recent progress in understanding the transition to turbulence in a pipe. *Nonlinearity* **18** (6), R17 (2005).

[14] KERSWELL, RR & TUTTY, OR Recurrence of travelling waves in transitional pipe flow. *Journal of Fluid Mechanics* **584**, 69–102 (2007).

[15] KHAPKO, T., DUGUET, Y., KREILOS, T., SCHLATTER, P., ECKHARDT, B. & HENNINGSON, D. S. Complexity of localised coherent structures in a boundary-layer flow. *Eur. Phys. J. E* **37** (32) (2013).

[16] KHAPKO, TARAS, KREILOS, TOBIAS, SCHLATTER, PHILIPP, DUGUET, YOHANN, ECKHARDT, BRUNO & HENNINGSON, DAN S Edge states as mediators of bypass transition in boundary-layer flows. *Journal of Fluid Mechanics* **801**, R2 (2016).

[17] KLEISER, L & SCHUMANN, UO Treatment of incompressibility and boundary conditions in 3-d numerical spectral simulations of plane channel flows. In *Proceedings of the Third GAMM–Conference on Numerical Methods in Fluid Mechanics*, pp. 165–173. Springer 1980.

[18] KREILOS, TOBIAS & ECKHARDT, BRUNO Periodic orbits near onset of chaos in plane couette flow. *Chaos: An Interdisciplinary Journal of Nonlinear Science* **22** (4), 047505 (2012).

[19] OLVERA, DANIEL & KERSWELL, RICH R. Optimising energy growth as a tool for finding exact coherent structures. *arXiv preprint arXiv:1701.09103* (2017).

[20] PANAGGIO, MARK J & ABRAMS, DANIEL M Chimera states: coexistence of coherence and incoherence in networks of coupled oscillators. *Nonlinearity* **28** (3), R67 (2015).

[21] PRINGLE, CHRIS CT, DUGUET, YOHANN & KERSWELL, RICH R Highly symmetric travelling waves in pipe flow. *Philosophical Transactions of the Royal Society of London A: Mathematical, Physical and Engineering Sciences* **367** (1888), 457–472 (2009).

[22] PYRAGAS, KESTUTIS Continuous control of chaos by self-controlling feedback. *Physics letters A* **170** (6), 421–428 (1992).

[23] RITTER, PAUL, MELLIBOVSKY, FERNANDO & AVILA, MARC Emergence of spatio-temporal dynamics from exact coherent solutions in pipe flow. *New Journal of Physics* **18** (8), 083031 (2016).

[24] SCHNEIDER, T. M., ECKHARDT, B. & YORKE, J. A. Turbulence transition and the edge of chaos in pipe flow. *Phys. Rev. Lett.* **99**, 034502 (2007).

[25] SCHNEIDER, TOBIAS M, GIBSON, JOHN F, LAGHA, MAHER, DE LILLO, FILIPPO & ECKHARDT, BRUNO Laminar-turbulent boundary in plane couette flow. *Physical Review E* **78** (3), 037301 (2008).

[26] SIEBER, JAN, OMEL'CHENKO, OLEH E & WOLFRUM, MATTHIAS Controlling unstable chaos: stabilizing chimera states by feedback. *Physical Review Letters* **112** (5), 054102 (2014).

[27] SKUFCA, J. D., YORKE, J. A. & ECKHARDT, B. Edge of chaos in a parallel shear flow. *Phys. Rev. Lett.* **96**, 174101 (2006).

[28] TAYLOR, JR, DEUSEBIO, E, CAULFIELD, CP & KERSWELL, RR A new method for isolating turbulent states in transitional stratified plane Couette flow. *Journal of Fluid Mechanics* **808**, R1 (2016).

[29] TUCKERMAN, LAURETTE S & BARKLEY, DWIGHT Bifurcation analysis for timesteppers. In *Numerical methods for bifurcation problems and large-scale dynamical systems*, pp. 453–466. Springer 2000.

[30] VISWANATH, DIVAKAR Recurrent motions within plane Couette turbulence. *Journal of Fluid Mechanics* **580**, 339–358 (2007).

[31] VYAZMINA, ELENA Bifurcations in a swirling flow. PhD thesis, École Polytechnique, France, 2010.

[32] WILLIS, ASHLEY P, CVITANOVIĆ, P & AVILA, MARC Revealing the state space of turbulent pipe flow by symmetry reduction. *Journal of Fluid Mechanics* **721**, 514–540 (2013).

[33] WILLIS, ASHLEY P, SHORT, KIMBERLY Y & CVITANOVIĆ, PREDRAG Symmetry reduction in high dimensions, illustrated in a turbulent pipe. *Physical Review E* **93** (2), 022204 (2016).

[34] WOLFRUM, MATTHIAS, OMEL'CHENKO, OLEH E & SIEBER, JAN Regular and irregular patterns of self-localized excitation in arrays of coupled phase oscillators. *Chaos: An Interdisciplinary Journal of Nonlinear Science* **25** (5), 053113 (2015).